Photoinduced Dynamics at the Water/TiO_2(101) Interface

Michael Wagstaffe,[1,*] Adrian Dominguez-Castro,[2] Lukas Wenthaus,[3] Steffen Palutke,[3] Dmytro Kutnyakhov,[3] Michael Heber,[3] Federico Pressacco,[3] Siarhei Dziarzhytski,[3] Helena Gleißner,[1,4,5] Verena Kristin Gupta,[2] Harald Redlin,[3] Adriel Dominguez,[2,6,7,8] Thomas Frauenheim,[2,6,7] Angel Rubio,[9,8,10,11] Andreas Stierle,[1,4,5,†] and Heshmat Noei[1,5]

[1]*Centre for X-ray and Nanoscience (CXNS), Deutsches Elektronen-Synchrotron (DESY), Notkestr. 85, 22607 Hamburg, Germany*
[2]*Bremen Center for Computational Material Science (BCCMS), University of Bremen, Am Fallturm 1, 28359 Bremen, Germany*
[3]*Deutsches Elektronen-Synchrotron (DESY), Notkestr. 85 D-22607, Hamburg, Germany*
[4]*Fachbereich Physik Universität Hamburg, Jungiusstr. 9-11, D-20355, Hamburg, Germany*
[5]*The Hamburg Centre for Ultrafast Imaging, Universität Hamburg, Luruper Chaussee 149, 22761 Hamburg, Germany*
[6]*Computational Science and Applied Research Institute (CSAR), 518110, Shenzhen, China*
[7]*Beijing Computational Science Research Center (CSRC), 100193, Beijing, China*
[8]*Nano-Bio Spectroscopy Group, Departamento de Fisica de Materiales, Universidad del País Vasco, UPV/EHU- 20018 San Sebastián, Spain*
[9]*Center for Free-Electron Laser Science, Deutsches Elektronen-Synchrotron DESY, Notkestr. 85, 22607 Hamburg, Germany*
[10]*Max Planck Institute for the Structure and Dynamics of Matter, Luruper Chaussee 149, 22761 Hamburg, Germany*
[11]*Center for Computational Quantum Physics, Flatiron Institute, New York 10010, New York, USA*

(Received 26 August 2022; accepted 17 January 2023; published 6 March 2023)

We present a femtosecond time-resolved optical pump-soft x-ray probe photoemission study in which we follow the dynamics of charge transfer at the interface of water and anatase TiO_2(101). By combining our observation of transient oxygen O 1*s* core level peak shifts at submonolayer water coverages with Ehrenfest molecular dynamics simulations we find that ultrafast interfacial hole transfer from TiO_2 to molecularly adsorbed water is completed within the 285 fs time resolution of the experiment. This is facilitated by the formation of a new hydrogen bond between an O_{2c} site at the surface and a physisorbed water molecule. The calculations fully corroborate our experimental observations and further suggest that this process is preceded by the efficient trapping of the hole at the surface of TiO_2 by hydroxyl species (-OH), that form following the dissociative adsorption of water. At a water coverage exceeding a monolayer, interfacial charge transfer is suppressed. Our findings are directly applicable to a wide range of photocatalytic systems in which water plays a critical role.

DOI: 10.1103/PhysRevLett.130.108001

Water is ubiquitous in nature and can heavily influence the surface chemistry at environmental interfaces; it can modify reaction pathways, hydrolyze reactants, alter the stability of adsorbed species and either enhance or inhibit surface reactivity [1]. Electron-hole pairs generated at the surface of TiO_2 are responsible for reactions used in technologies for air and water purification, self cleaning surfaces and hydrogen production [2–9]. The photochemical splitting of water [6], in particular, is an environmentally benign strategy for carbon-free fuel production important for our future hydrogen based economy. Despite the many studies dedicated to understanding the underlying photochemistry, the reaction sequence remains unclear. This is partly due to a lack of direct experimental evidence in unraveling the ultrafast dynamics during the initial stages of these complex multielectron processes.

While it is generally accepted that water adsorbs on anatase (101) to form a mixture of physisorbed H_2O and chemisorbed OH species [10,11], the precise nature of charge trapping, interfacial charge transfer, the relative importance of the different intermediate species that form along competing reaction channels during photocatalysis and the interplay thereof with charge carrier recombination (ranging from picoseconds to microseconds [4]) remain widely debated [12]. Theoretical studies highlight the importance of ultrafast hole trapping at surface active sites in facilitating water splitting [8,13–16], but often conflictingly suggest that holes are trapped at either Ti interstitials [15], bridging O atoms [8,16], or at surface hydroxyl species [8,13]. The relative competition of the H_2O-H_2O and H_2O-TiO_2 interactions influences the dynamics of water dissociation, raising questions about the importance of hydrogen bonding at the interface on the efficiency of interfacial charge transfer [17–19]. Geng *et al.*[18] investigated photoinduced water dissociation on anatase TiO_2(101), initiated by a 266 nm femtosecond laser pulse (70 mW/cm^2). Contrary to rutile [20], on which water dissociation is suppressed at higher water coverages, the dissociation probability appeared independent of coverage. This is thought to be a consequence of the weaker interactions

between surface water molecules due to the larger distance between neighboring Ti_{5c} sites on anatase (101), meaning that at submonolayer coverages no hydrogen bonds between water molecules are present [21]. This suggests that strong hydrogen bonding networks can be detrimental to efficient water splitting. In contrast, on anatase-$TiO_2(001)$ the formation of a hydrogen-bond network above one monolayer promoted water splitting by providing a cascaded channel for hole transfer to water [19].

Various time resolved studies on TiO_2 are reported, in which focus is often placed on electron-hole trapping and recombination dynamics, using techniques such as transient absorption spectroscopy [22–24] and x-ray absorption spectroscopy [25,26]. Though these studies have provided valuable insight down to the femtosecond regime, they typically lack high chemical and surface sensitivity that is necessary for a comprehensive understanding of the early stage photoinduced dynamics. Here, we probe the photoinduced dynamics taking place within the initial several picoseconds following photoexcitation at the interface of H_2O and anatase $TiO_2(101)$ with high chemical and surface sensitivity using ultrafast optical pump-soft x-ray probe photoemission spectroscopy combined with Ehrenfest molecular dynamics simulations. Our study highlights the role of surface hydroxide species and the influence of hydrogen bonding in potential charge transfer pathways, revealing that strong hydrogen bond formation between the anatase (101) surface and H_2O molecules is conducive to efficient charge separation.

The experiment was carried out at the plane grating monochromator beam line PG2 [27,28] of the free-electron laser in Hamburg (FLASH) at the Deutsches Elektronen-Synchrotron (DESY) [29,30]. X-ray free-electron lasers (FELs) are instrumental for understanding reaction dynamics on their natural timescales [31–36]. FLASH provided a pulse pattern of bursts with 10 Hz repetition rate, each burst consisting of 400 single soft x-ray pulses with a 1 MHz repetition rate and fundamental pulse energies of 30–40 μJ. The third harmonic ($h\nu_{FEL} = 645$ eV) was synchronized with an optical laser ($h\nu_{opt} = 1.6$ eV) to pump the photocatalytic reaction via two-photon excitation (TPE). The $TiO_2(101)$ surface was prepared by cycles of Ar^+ ion sputtering and annealing in oxygen to create a clean and well-ordered surface. Annealing in oxygen establishes a nearly defect-free surface. This minimizes the presence of intragap states arising due to oxygen vacancy-induced bulk Ti polarons [37], resulting in mainly TPE at this energy. For more details refer to Supplemental Material S1 [38] for the experimental section [5,27–32,39–52]. The experimental temporal resolution of 285 ± 9 fs was determined by measuring the transient formation and decay of sidebands that are present when the pump and probe pulses overlap. This is described in [53] and discussed in Fig. S2 of the Supplemental Material [38].

Figure 1 shows the laser induced dynamics of the O 1*s* core level for the TiO_2 surface before and during water exposure, (a) and (b), respectively. In each case (i) corresponds to the time-resolved XPS map of the O 1*s* core level recorded during the experiment with (iii) displaying it as a series of 2D core level spectra averaged over 1.2 ps windows. In both cases, (ii) displays a pair of integrated intensity plots as a function of delay time taken from the high (red) and low (blue) binding energy (BE) side of the O 1*s* peak of lattice oxygen in (i) (with corresponding areas highlighted atop the core level map). Similarly, difference spectra in (iv) taken from the pre-pumped region highlight any transient changes, sacrificing temporal resolution for improved energy resolution. For the clean surface recorded in ultrahigh vacuum at 295 K, (a), the O 1*s* spectra comprise of a single peak at 530.4 eV, assigned to lattice oxygen in TiO_2. Other than the expected sidebands at time zero, no laser-induced changes are observed. Previous time-resolved pump-probe photoemission studies [32,54] demonstrated that following charge carrier generation the O 1*s* and the Ti 2*p* core levels can experience BE shifts of up to −0.2 eV. This is a result of the surface photovoltage (SPV) effect, which causes transient shifts of the substrate related core levels as the photogenerated charge carriers move to reduce the intrinsic band bending [5,55,56] and bring the system back to a flat band condition [4,5,32,54–59]. This is discussed further in S3 [38]. The negative BE shift reflects a movement away from downward bent bands, typical for vacuum prepared TiO_2 [5]. The absence of any SPV induced shifts on our clean surface is likely a result of preparation in oxygen. This was intended to minimize the intrinsic band bending by ensuring a negligible defect concentration in the near surface region. These data highlight the absence of any resolvable changes induced by the laser on the bare substrate, acting as a control experiment prior to the introduction of water.

Next, the clean $TiO_2(101)$ surface was studied under a constant back pressure of H_2O (3.10^{-8} mbar) to investigate the water mediated dynamics *in situ*. A submonolayer coverage of water was maintained to maximize probing of the water-oxide interface and to minimize water-water interactions [21]. This was achieved by tailoring the laser power and temperature to 6.6 mJ/cm^2 and 160 K, respectively, which gave an estimated coverage of ≤80% of the first monolayer, i.e., water only bound to fivefold Ti sites [60,61]. Figure S4 [38], displays the data in Fig. 1(a) averaged over the entire temporal window and demonstrates that exposure of anatase $TiO_2(101)$ to water results in mixed molecular and dissociative adsorption, forming surface hydroxyl species, in line with previous reports [10,11]. This leads to an increase in downwards band bending and a positive BE shift of the core level peaks [10,55,62–64], as highlighted in Fig. S5 [38]. For a discussion of how the coverage was estimated [11,60,61], see Fig. S6 [38].

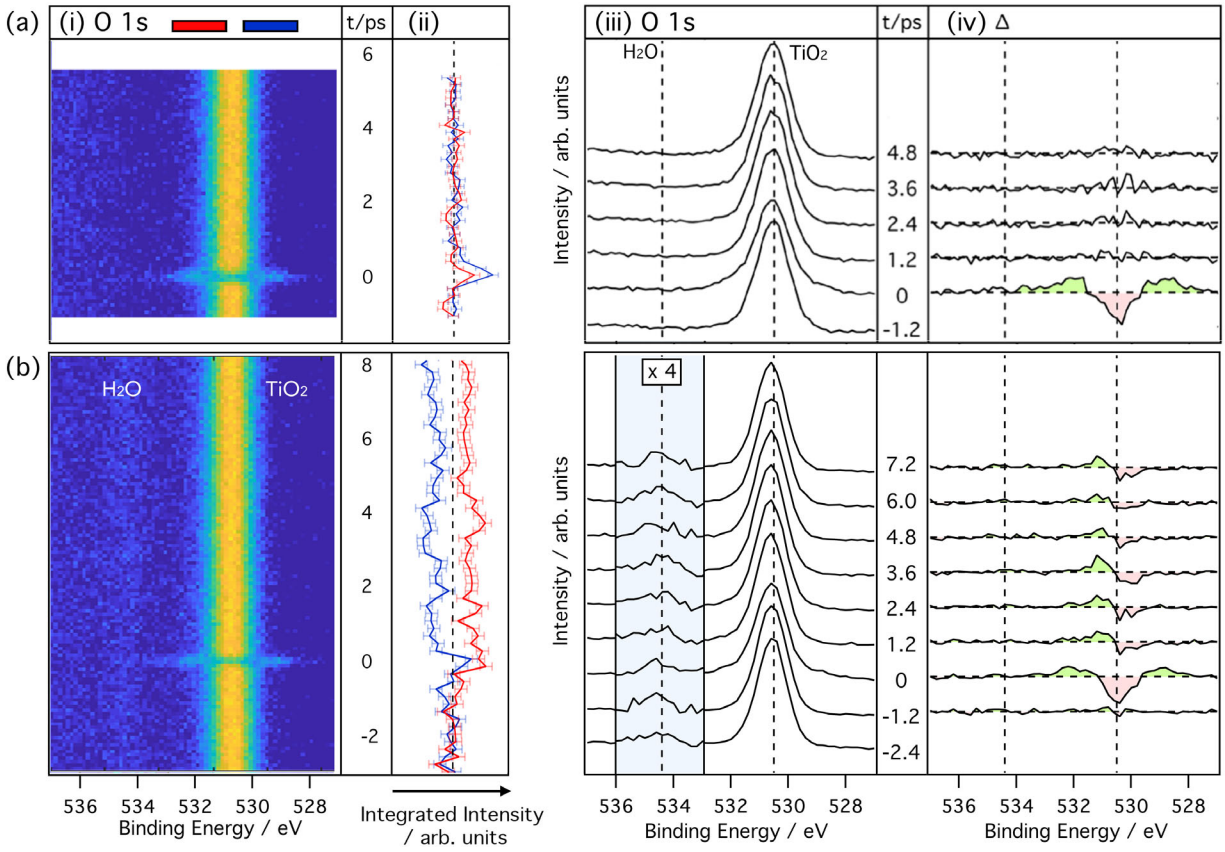

FIG. 1. Time-resolved XP spectra of (a) $TiO_2(101)$ ($T = 295$ K) and (b) $H_2O/TiO_2(101)$ ($T = 160$ K). (i) O1s XPS map recorded during the pump probe experiment between −3.0 and 8.0 ps (a) clean (b) H_2O covered surface (ii) integrated intensity, as a function of delay time, in which the colors correspond to the regions marked in the header of the XPS map. The associated error bars were determined by monitoring variations of the intensities in the pre-pumped region before time zero, during which no change is expected. (iii) O 1*s* core level spectra from (i), (iv) corresponding difference spectra, taken from the pre-pumped region at—1.2 ps in (a) and at −2.4 ps in (b).

In Fig. 1(b) a 50 meV positive BE shift of the lattice oxide component at 530.5 eV is evident instantaneously after photoexcitation of water covered TiO_2. This shift is seen in the integrated intensity plot, Fig. 1(b)(ii), via an intensity increase at the higher BE side of the lattice oxide peak (red line) with a corresponding decrease at the lower BE side (blue line). The absolute value of the shift was obtained by considering the amplitude of the difference signals displayed in 1(b)(iv), shown in S7 of the Supplemental Material [38]. The fitting results for the lattice oxide component are included in S8 [38], which highlights that no change in the FWHM of the peak is observed during the measurement [55,57]. Figure S9 [38] overlays the two integrated intensity plots to further highlight the differences in the photoinduced dynamics on the clean surface and water covered TiO_2 [31,32]. Figure 2 displays the transient change of the O 1*s* peak associated with physisorbed water at 534.6 eV. Because of the low coverage, extracting reliable information with both a high energy and high temporal resolution is not possible. To account for this, the signals before and after time zero were averaged over 2.4 and 7.2 ps windows, respectively. The resultant spectra are shown in Fig. 2(a). By doing this, we assume that all changes occur within the first 285 fs, which, based on the behavior of the lattice oxide component, is reasonable. Following illumination, the peak experiences broadening to lower BE, with an overall increase in the

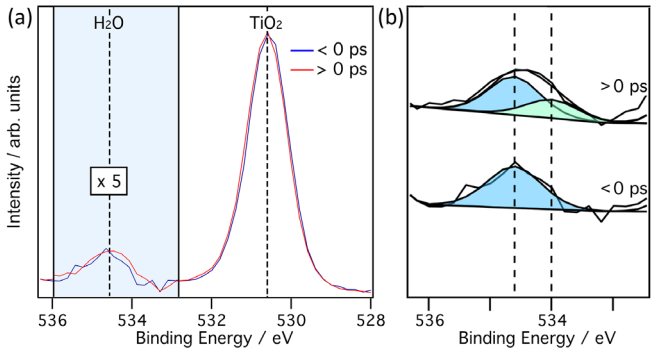

FIG. 2. (a) Time resolved O 1*s* XP spectra of the $H_2O/TiO_2(101)$ system before (blue) and after (red) laser excitation ($T = 160$ K) averaged over 2.4 and 7.2 ps windows, respectively. In (b) are the fits of the H_2O component.

FWHM of the envelope of 20%. As shown in Fig. 2(b), for a satisfactory fit this necessitates a second component at 534.0 eV, $\Delta E = -0.6$ eV, the origin of which is discussed later. The overall intensity in the H_2O region remains constant with respect to the lattice oxide component. This allows us to rule out desorption related effects as the reason for the observed core-level peak shifts.

These transient changes are indicative of a photoinduced redistribution of charge at the interface which leads to changes in the degree of band bending [57]. This manifests itself as a transient BE shift of the substrate related O 1s core level peak [55–57,65–67]. A change in surface band bending is already observed upon H_2O adsorption (Fig. S5 in the Supplemental Material [38]), as electron transfer equilibrium was established and the molecule and substrate bands aligned. Here, a transient positive BE shift of the lattice oxide component allows us to infer that there is an increase in downward band bending. The direction of the shift allows us to rule out the SPV effect [32,54]. Since this shift was not observed in the prepumped region (< 0 ps), nor on the bare substrate, it can only be assigned to photoinduced hole transfer from the valence band of TiO_2 to water, immediately following the generation of electron hole pairs. The persistent core level shift allows us to further clarify that rapid back transfer of an electron from TiO_2 to water (typically considered detrimental to solar light harvesting [9]) does not take place for at least 8 ps, with the hole remaining trapped in H_2O. Subtle lattice distortions that might take place upon bond formation or charge transfer have also been shown to contribute to a so-called effective shift in binding energy of the atomic core levels at the surface [68]. However, any structural changes that could lead to a shift induced by the laser and subsequent electron hole pair generation have already been excluded by investigating the clean surface [Fig. 1(a)] and our theoretical simulations, discussed in the following section, show no evidence of any structural changes to the TiO_2 lattice throughout the experiment. Further, the consistent line profile and FWHM of the lattice oxide O 1s component before and after illumination suggests that band bending induced shifts are at least for the most part responsible for the observed peak shift. This is discussed further in Supplemental Material S8 [38].

To support our experimental observation and to describe the behavior of the charge carriers in the early stages, we turn to our density-functional-tight binding (DFTB) calculations. We studied many adsorption configurations and their effects on the photochemistry of $H_2O/TiO_2(101)$ [43,45,69–71]. Upon adsorption no intragap states appear and thus no new bands are expected in the absorption spectrum. For a full discussion of the adsorption geometries and energies and their corresponding density of states see S10 and S11. The calculated O 1s core level XPS binding energies for molecular and mixed adsorption [46–52,72] are included in Table S12 [38]. Pertinent to our case, the density of states results show that no significant changes appear when water adsorbs molecularly on $TiO_2(101)$, similar to a previous report [15]. The dissociated molecules, however, present significant hybridization of the OH terminal group with the O 2p states of the surface at the top of the valence band. This could facilitate efficient charge separation and trapping of the photogenerated holes at OH sites, leading to the formation of a hydroxyl radical ($^{\bullet}$OH) [73–75] and inhibiting charge carrier recombination.

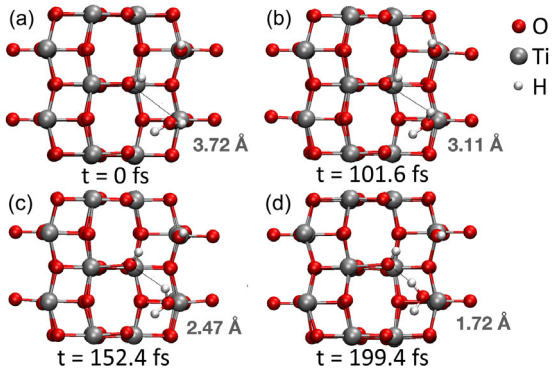

FIG. 3. Dynamic evolution for H_2O adsorbed over Ti5c and a partially hydroxylated surface. (a) 0; (b) 101.6; (c) 152.4; (d) 199.4 fs.

The dynamics taking place during the first 200 fs after illumination were studied in an Ehrenfest simulation using a 3.245 eV laser pulse (corresponding to TPE) with a pulse duration of 20 fs [76], shown in Fig. S13 in the Supplemental Material [38]. For mixed molecular and dissociative adsorption a net charge transfer from water to TiO_2 is observed during the simulation. Figure 3 presents the evolution of the dynamics for a H_2O molecule adsorbed over a Ti_{5c} site and a hydroxylated surface. Following irradiation a new hydrogen bond forms between a hydrogen atom in physisorbed water and an O_{2c} site, reducing the initial O$\cdots$H bond distance of 3.72 to 1.72 Å, after 199.4 fs, see movie S1 in the Supplemental Material [38]. The formation of this new hydrogen bond at submonolayer coverages between Ti-OH and H_2O facilitates efficient charge transfer to water, following the trapping of a hole at the surface due to the presence of surface hybridized states.

We calculated the O 1s binding energies before and after light illumination and compared them to the experimental peak positions [46–49] in Table S14 [38]. When considering the associated errors [72], we find very good agreement in both the magnitude and direction of the core level shifts. Our simulations show that laser illumination and the subsequent geometrical rearrangement induces a positive 0.1 eV shift of the lattice oxide peak and a negative 0.9 eV shift of the H_2O peak. All substrate related surface oxygen atoms experience an equivalent shift, further supporting the interpretation that the measured shift is due to changes in surface band bending rather than structural distortions of

individual surface O atoms. The O 1s binding energies of water have been theoretically shown to correlate with the structural properties of the hydrogen-bonding network [61]. The increase in the intramolecular hydrogen-oxygen bond length induced following the formation of new hydrogen bonds with neighbouring molecules may lead to a considerable reduction in the BE of the corresponding oxygen species. Furthermore, previous calculations reveal a linear correlation between the length of the O···H hydrogen bond in water clusters and the core level BE. The formation of new hydrogen bonds, and the resulting physisorbed H_2O species with a reduced O···H bond length, results in a shift of the BE to lower values and is the origin of the new component observed at 534.0 eV. The presence of two H_2O components in our experimental data suggests that not all H_2O molecules are involved in bond formation and hole trapping. This can also explain the difference between the experimentally observed 50 meV shift and the predicted 100 meV shift of the lattice oxide component. The simulations consider a somewhat simplified case where all water molecules are involved, leading to a rigid shift of the entire H_2O related component. The magnitude of the shift attributed to changes in surface band bending is directly linked to the extent of charge redistribution. Physisorbed water molecules that do not interact with a hole trapped at surface sites will not be involved in a charge transfer process and thus not contribute to a band bending induced shift. This leads to a comparatively smaller shift, as we experimentally observe. A preliminary investigation at higher water coverages revealed that at coverages exceeding a monolayer, no laser-induced changes are observed. This is displayed in Fig. S15 of the Supplemental Material [38] and shows that at higher coverages the charge transfer process is suppressed [60,61]. This is likely due to the stronger water-water interactions, supporting that strong interwater hydrogen bonding networks over the TiO_2 surface can suppress interfacial charge transfer and inhibit the photocatalytic process [21].

Our results provide new insight into the important role of the adsorption state of water molecules at the surface of TiO_2 and the influence of hydrogen bonding in potential charge-transfer pathways for the rate-limiting steps taking place within the first several hundred femtoseconds during photocatalysis. Upon photoexcitation, water molecules in the first layer strongly interact with the titania surface to form hydrogen bonds which facilitate the interfacial transfer photogenerated holes within 285 fs, effectively competing with timescales expected for electron-hole recombination. This is preceded by the efficient localization of holes at hydroxide species at the surface, formed following the dissociative adsorption of water. As coverage increases the probability of interfacial charge transfer is suppressed, likely owing to water molecules in the first layer interacting with those in the multilayer, thereby weakening the interaction of the former with the surface and reducing the hole trapping capability. Unraveling these ultrafast dynamics and identifying the timescale and mechanism of the individual reaction steps is a prerequisite for the development of tailored systems for water splitting (and catalysts in general) with improved activity and selectivity. We obtain unique insight into the photoinduced dynamics taking place at the interface of H_2O and $TiO_2(101)$ during the initial, rate-determining, steps relevant to a range of photocatalytic systems. In doing so we highlight the possibilities of soft x-ray FELs to directly probe photoinduced dynamics.

M. W. acknowledges support from the Initiative and Networking Funds of the Helmholtz Association through ExNet-0002. This work is supported by the Cluster of Excellence "CUI: Advanced Imaging of Matter" of the Deutsche Forschungsgemeinschaft (DFG)—EXC 2056—project ID 390715994. A. D. C. would like to thank Dr. Mauricio Chagas da Silva for the fruitful discussions. A. D. C. wishes to acknowledge funding by DFG-RTG2247 grant (RTG-QM3 Program) for the doctoral fellowship, and computational resources at BCCMS, University of Bremen. A. D. and A. R. acknowledge financial support from the European Union's Horizon 2020 research and innovation program under Marie Sklodowska-Curie Grant Agreement No. 753874 and from the European Research Council (ERC-2015-AdG-694097), Grupos Consolidados (IT1249-19), and SFB925. T. F. and A. D. acknowledge financial support from NSAF U1930402 and computational resources from the Beijing Computational Science Research Center. We acknowledge DESY (Hamburg, Germany), a member of the Helmholtz Association HGF, for the provision of experimental facilities. Parts of this research were carried out at FLASH and the DESY NanoLab and we would like to acknowledge the excellent support from the scientific and technical staff of both facilities and thank Dr. Rolf Treusch for the useful discussions. Beam time was allocated for proposal F-20181204.

*Corresponding author.
michael.wagstaffe@desy.de
†Corresponding author.
andreas.stierle@desy.de

[1] G. Rubasinghege and V. H. Grassian, Role(s) of adsorbed water in the surface chemistry of environmental interfaces, Chem. Commun. **49**, 3071 (2013).
[2] R. Qian, H. Zong, J. Schneider, G. Zhou, T. Zhao, Y. Li, J. Yang, D. W. Bahnemann, and J. H. Pan, Charge carrier trapping, recombination and transfer during TiO_2 photocatalysis: An overview, Catal. Today **335**, 78 (2019).
[3] S. Kohtani, A. Kawashima, and H. Miyabe, Reactivity of trapped and accumulated electrons in titanium dioxide photocatalysis, Catal. Chem. **7**, 303 (2017).
[4] J. Schneider, M. Matsuoka, M. Takeuchi, J. Zhang, Y. Horiuchi, M. Anpo, and D. W. Bahnemann, Understanding TiO_2 photocatalysis: Mechanisms and materials, Chem. Rev. **114**, 9919 (2014).

[5] U. Diebold, The surface science of titanium dioxide, Surf. Sci. Rep. **48**, 53 (2003).
[6] A. Fujishima and K. Honda, Electrochemical photolysis of water at a semiconductor electrode, Nature (London) **238**, 37 (1972).
[7] B. O'Regan and M. Grätzel, A low-cost, high-efficiency solar cell based on dye-sensitized colloidal TiO_2 films, Nature (London) **353**, 737 (1991).
[8] A. Migani and L. Blancafort, What controls photocatalytic water oxidation on rutile $TiO_2(110)$ under ultra-high-vacuum conditions?, J. Am. Chem. Soc. **139**, 11845 (2017).
[9] M. A. Henderson, A surface science perspective on TiO_2 photocatalysis, Surf. Sci. Rep. **66**, 185 (2011).
[10] L. E. Walle, A. Borg, E. M. J. Johansson, S. Plogmaker, H. Rensmo, P. Uvdal, and A. Sandell, Mixed dissociative and molecular water adsorption on anatase $TiO_2(101)$, J. Phys. Chem. C **115**, 9545 (2011).
[11] M. J. Jackman, A. G. Thomas, and C. Muryn, Photoelectron spectroscopy study of stoichiometric and reduced anatase $TiO_2(101)$ surfaces: The effect of subsurface defects on water adsorption at near-ambient pressures, J. Phys. Chem. C **119**, 13682 (2015).
[12] J. Zhang and Y. Nosaka, Mechanism of the OH radical generation in photocatalysis with TiO_2 of different crystalline types, J. Phys. Chem. C **118**, 10824 (2014).
[13] G. Odling and N. Robertson, Why is anatase a better photocatalyst than rutile? The importance of free hydroxyl radicals, ChemSusChem **8**, 1838 (2015).
[14] K. Shirai, G. Fazio, T. Sugimoto, D. Selli, L. Ferraro, K. Watanabe, M. Haruta, B. Ohtani, H. Kurata, C. Di Valentin, and Y. Matsumoto, Water-assisted hole trapping at the highly curved surface of nano-TiO_2 photocatalyst, J. Am. Chem. Soc. **140**, 1415 (2018).
[15] G. A. Tritsaris, D. Vinichenko, G. Kolesov, C. M. Friend, and E. Kaxiras, Dynamics of the photogenerated hole at the rutile $TiO_2(110)$/water interface: A nonadiabatic simulation study, J. Phys. Chem. C **118**, 27393 (2014).
[16] C. Di Valentin, A mechanism for the hole-mediated water photooxidation on $TiO_2(101)$ surfaces, J. Phys. Condens. Matter **28**, 074002 (2016).
[17] K. Shirai, T. Sugimoto, K. Watanabe, M. Haruta, H. Kurata, and Y. Matsumoto, Effect of water adsorption on carrier trapping dynamics at the surface of anatase TiO_2 nanoparticles, Nano Lett. **16**, 1323 (2016).
[18] Z. Geng, X. Chen, W. Yang, Q. Guo, C. Xu, D. Dai, and X. Yang, Highly efficient water dissociation on anatase $TiO_2(101)$, J. Phys. Chem. C **120**, 26807 (2016).
[19] X. Ma, Y. Shi, J. Liu, X. Li, X. Cui, S. Tan, J. Zhao, and B. Wang, Hydrogen-bond network promotes water splitting on the TiO_2 surface, J. Am. Chem. Soc. **144**, 13565 (2022).
[20] W. Yang, D. Wei, X. Jin, C. Xu, Z. Geng, Q. Guo, Z. Ma, D. Dai, H. Fan, and X. Yang, Effect of the hydrogen bond in photoinduced water dissociation: A double-edged sword, J. Phys. Chem. Lett. **7**, 603 (2016).
[21] A. Tilocca and A. Selloni, Vertical and lateral order in adsorbed water layers on anatase $TiO_2(101)$, Langmuir **20**, 8379 (2004).
[22] Y. Tamaki, A. Furube, M. Murai, K. Hara, R. Katoh, and M. Tachiya, Dynamics of efficient electron–hole separation in TiO_2 nanoparticles revealed by femtosecond transient absorption spectroscopy under the weak-excitation condition, Phys. Chem. Chem. Phys. **9**, 1453 (2007).
[23] Y. Tamaki, K. Hara, R. Katoh, M. Tachiya, and A. Furube, Femtosecond visible-to-ir spectroscopy of TiO_2 nanocrystalline films: Elucidation of the electron mobility before deep trapping, J. Phys. Chem. C **113**, 11741 (2009).
[24] B. Enright and D. Fitzmaurice, Spectroscopic determination of electron and hole effective masses in a nanocrystalline semiconductor film, J. Phys. Chem. **100**, 1027 (1996).
[25] Y. Obara, H. Ito, T. Ito, N. Kurahashi, S. Thürmer, H. Tanaka, T. Katayama, T. Togashi, S. Owada, Y.-i. Yamamoto, S. Karashima, J. Nishitani, M. Yabashi, T. Suzuki, and K. Misawa, Femtosecond time-resolved x-ray absorption spectroscopy of anatase TiO_2 nanoparticles using XFEL, Struct. Dyn. **4**, 044033 (2017).
[26] S. H. Park, A. Katoch, K. H. Chae, S. Gautam, P. Miedema, S. W. Cho, M. Kim, R.-P. Wang, M. Lazemi, F. de Groot, and S. Kwon, Direct and real-time observation of hole transport dynamics in anatase TiO_2 using x-ray free-electron laser, Nat. Commun. **13**, 2531 (2022).
[27] M. Martins, M. Wellhöfer, J. T. Hoeft, W. Wurth, J. Feldhaus, and R. Follath, Monochromator beamline for FLASH, Rev. Sci. Instrum. **77**, 115108 (2006).
[28] N. Gerasimova, S. Dziarzhytski, and J. Feldhaus, The monochromator beamline at FLASH: Performance, capabilities and upgrade plans, J. Mod. Opt. **58**, 1480 (2011).
[29] S. Toleikis, The FLASH facility current status in 2018 and future upgrade plans, AIP Conf. Proc. **2054**, 030015 (2019).
[30] W. Ackermann *et al.*, Operation of a free-electron laser from the extreme ultraviolet to the water window, Nat. Photonics **1**, 336 (2007).
[31] M. Wagstaffe, L. Wenthaus, A. Dominguez-Castro, S. Chung, G. D. Lana Semione, S. Palutke, G. Mercurio, S. Dziarzhytski, H. Redlin, N. Klemke, Y. Yang, T. Frauenheim, A. Dominguez, F. Kärtner, A. Rubio, W. Wurth, A. Stierle, and H. Noei, Ultrafast real-time dynamics of co oxidation over an oxide photocatalyst, ACS Catal. **10**, 13650 (2020).
[32] K. Ozawa, M. Emori, S. Yamamoto, R. Yukawa, S. Yamamoto, R. Hobara, K. Fujikawa, H. Sakama, and I. Matsuda, Electron-hole recombination time at TiO_2 single-crystal surfaces: Influence of surface band bending, J. Phys. Chem. Lett. **5**, 1953 (2014).
[33] H. Öström *et al.*, Probing the transition state region in catalytic CO oxidation on Ru, Science **347**, 978 (2015).
[34] M. Beye *et al.*, Selective Ultrafast Probing of Transient Hot Chemisorbed and Precursor States of CO on Ru(0001), Phys. Rev. Lett. **110**, 186101 (2013).
[35] A. P. Mancuso *et al.*, Coherent imaging of biological samples with femtosecond pulses at the free-electron laser FLASH, New J. Phys. **12**, 035003 (2010).
[36] C. Gahl, A. Azima, M. Beye, M. Deppe, K. Döbrich, U. Hasslinger, F. Hennies, A. Melnikov, M. Nagasono, A. Pietzsch, M. Wolf, W. Wurth, and A. Föhlisch, A femtosecond x-ray/optical cross-correlator, Nat. Photonics **2**, 165 (2008).
[37] B. Liu, X. Zhao, J. Yu, I. P. Parkin, A. Fujishima, and K. Nakata, Intrinsic intermediate gap states of TiO_2 materials and their roles in charge carrier kinetics, J. Photochem. Photobiol. C **39**, 1 (2019).

[38] See Supplemental Material at http://link.aps.org/supplemental/10.1103/PhysRevLett.130.108001 for. S1: Experimental method and computational details; S2: time resolved XPS map of the Ti $2p_{3/2}$ core level as a function of delay time (a), with a corresponding integrated intensity plot over time zero (b); S3: Time resolved XP spectra for the as-prepared $TiO_2(101)$ system as a function of delay time with corresponding integrated intensity plots. (b) spectra extracted in 1.2 ps windows; S4: time averaged XP spectra showing the coverage of water; S5: Core level O 1*s* spectra following the adsorption of sub-monolayer and multilayer water on the TiO_2 anatase (101) surface. S6: Time averaged data for the O 1*s* core level at different coverages used to quantify the coverage of water; S7: A comparison of the experimental difference spectrum with modeled difference spectra resulting from different core level peak shifts; S8: Fitting results (FWHM and peak position) from the time resolved spectra in S3 (b); S9: An overlay of two integrated intensity plots shown in Figure 1; S10 and S11: DFTB calculations describing the electronic and structural properties of the adsorption; S12: Calculated O 1*s* core level XPS binding energies pertaining to H2O adsorbed on anatase $TiO_2(101)$; S13: Ehrenfest dynamics simulation studying the changes in the Mulliken charges with respect to their ground-state values as a function of time. S14: Calculated O 1*s* core level XPS binding energies before and after light illumination; S15: Time-averaged core level O 1*s* spectra for higher water coverage during our experiment, with the corresponding time resolved integrated intensity. Movie S1: Movie showing simulated hydrogen bond formation during the first 199.4 fs.

[39] M. Watanabe and T. Hayashi, Time-resolved study of self-trapped exciton luminescence in anatase TiO_2 under two-photon excitation, J. Lumin. **112**, 88 (2005).

[40] L. Wenthaus, A. Benz, S. Palutke, D. Kutnyakhov, H. Meyer, S. Gieschen, and M. Beye, Double electron spectrometer setup for time-resolved photoelectron spectroscopy at a free-electron laser (to be published).

[41] P. K. Samanta and N. J. English, Opto-electronic properties of stable blue photosensitisers on a TiO_2 anatase-101 surface for efficient dye-sensitised solar cells, Chem. Phys. Lett. **731**, 136624 (2019) .

[42] B. Aradi, B. Hourahine, and T. Frauenheim, DFTB+, a sparse matrix-based implementation of the DFTB method, J. Phys. Chem. A **111**, 5678 (2007).

[43] D. Selli, G. Fazio, G. Seifert, and C. Di Valentin, Water multilayers on $TiO_2(101)$ anatase surface: Assessment of a DFTB-based method, J. Chem. Theory Comput. **13**, 3862 (2017).

[44] F. P. Bonafé, B. Aradi, M. Guan, O. A. Douglas-Gallardo, C. Lian, S. Meng, T. Frauenheim, and C. G. Sánchez, Plasmon-driven sub-picosecond breathing of metal nanoparticles, Nanoscale **9**, 12391 (2017).

[45] F. P. Bonafé, F. J. Hernández, B. Aradi, T. Frauenheim, and C. G. Sánchez, Fully atomistic real-time simulations of transient absorption spectroscopy, J. Phys. Chem. Lett. **9**, 4355 (2018).

[46] G. Kresse and J. Furthmüller, Efficiency of *ab-initio* total energy calculations for metals and semiconductors using a plane-wave basis set, Comput. Mater. Sci. **6**, 15 (1996).

[47] G. Kresse and J. Furthmüller, Efficient iterative schemes for ab initio total-energy calculations using a plane-wave basis set, Phys. Rev. B **54**, 11169 (1996).

[48] G. Kresse and J. Hafner, *Ab initio* molecular dynamics for liquid metals, Phys. Rev. B **47**, 558 (1993).

[49] G. Kresse and J. Hafner, Ab initio molecular-dynamics simulation of the liquid-metal–amorphous-semiconductor transition in germanium, Phys. Rev. B **49**, 14251 (1994).

[50] J. P. Perdew, M. Ernzerhof, and K. Burke, Rationale for mixing exact exchange with density functional approximations, J. Chem. Phys. **105**, 9982 (1996).

[51] P. E. Blöchl, Projector augmented-wave method, Phys. Rev. B **50**, 17953 (1994).

[52] G. Kresse and D. Joubert, From ultrasoft pseudopotentials to the projector augmented-wave method, Phys. Rev. B **59**, 1758 (1999).

[53] A. Pietzsch, A. Föhlisch, M. Beye, M. Deppe, F. Hennies, M. Nagasono, E. Suljoti, W. Wurth, C. Gahl, K. Döbrich, and A. Melnikov, Towards time resolved core level photoelectron spectroscopy with femtosecond x-ray free-electron lasers, New J. Phys. **10**, 033004 (2008).

[54] Y. Zhang, D. T. Payne, C. L. Pang, C. Cacho, R. T. Chapman, E. Springate, H. H. Fielding, and G. Thornton, State-selective dynamics of TiO_2 charge-carrier trapping and recombination, J. Phys. Chem. Lett. **10**, 5265 (2019).

[55] C. T. Campbell, Ultrathin metal films and particles on oxide surfaces: Structural, electronic and chemisorptive properties, Surf. Sci. Rep. **27**, 1 (1997).

[56] K. L. Syres, A. G. Thomas, W. R. Flavell, B. F. Spencer, F. Bondino, M. Malvestuto, A. Preobrajenski, and M. Grätzel, Adsorbate-induced modification of surface electronic structure: Pyrocatechol adsorption on the anatase TiO_2 (101) and rutile TiO_2 (110) surfaces, J. Phys. Chem. C **116**, 23515 (2012).

[57] Z. Zhang and J. T. Yates, Band bending in semiconductors: Chemical and physical consequences at surfaces and interfaces, Chem. Rev. **112**, 5520 (2012).

[58] J. O'Connor, B. A. Sexton, and R. S. C. Smart, *Surface Analysis Methods in Materials Science* (Springer, New York, 2003), Vol. 23.

[59] M. P. Seah and W. A. Dench, Quantitative electron spectroscopy of surfaces: A standard data base for electron inelastic mean free paths in solids, Surf. Interface Anal. **1**, 2 (1979).

[60] G. S. Herman, Z. Dohnálek, N. Ruzycki, and U. Diebold, Experimental investigation of the interaction of water and methanol with anatase-$TiO_2(101)$, J. Phys. Chem. B **107**, 2788 (2003).

[61] P. Aplincourt, C. Bureau, J.-L. Anthoine, and D. P. Chong, Accurate density functional calculations of core electron binding energies on hydrogen-bonded systems, J. Phys. Chem. A **105**, 7364 (2001).

[62] M. B. Hugenschmidt, L. Gamble, and C. T. Campbell, The interaction of H_2O with a $TiO_2(110)$ surface, Surf. Sci. **302**, 329 (1994).

[63] S. Kashiwaya, J. Morasch, V. Streibel, T. Toupance, W. Jaegermann, and A. Klein, The work function of TiO_2, Surfaces **1**, 73 (2018).

[64] A. Stierle, T. F. Keller, H. Noei, V. Vonk, and R. Roehlsberger, Desy nanolab, J. Large-Scale Res. Facil. **2** (2016).

[65] S. Porsgaard, P. Jiang, F. Borondics, S. Wendt, Z. Liu, H. Bluhm, F. Besenbacher, and M. Salmeron, Charge state of gold nanoparticles supported on titania under oxygen pressure, Angew. Chem., Int. Ed. **50**, 2266 (2011).

[66] M. Setvin, J. Hulva, G. S. Parkinson, M. Schmid, and U. Diebold, Electron transfer between anatase TiO_2 and an O_2 molecule directly observed by atomic force microscopy, Proc. Natl. Acad. Sci. U.S.A. **114**, E2556 (2017).

[67] K. Syres, A. Thomas, F. Bondino, M. Malvestuto, and M. Grätzel, Dopamine adsorption on anatase $TiO_2(101)$: A photoemission and NEXAFS spectroscopy study, Langmuir **26**, 14548 (2010).

[68] E. Gränäs, M. Busch, B. Arndt, M. Creutzburg, G. D. L. Semione, J. Gustafson, A. Schaefer, V. Vonk, H. Grönbeck, and A. Stierle, Role of hydroxylation for the atomic structure of a non-polar vicinal zinc oxide, Commun. Ser. B **4**, 1 (2021).

[69] S. Rhatigan and M. Nolan, Activation of water on MnO_x-nanocluster-modified rutile (110) and anatase (101) TiO_2 and the role of cation reduction, Front. Chem. **7**, 67 (2019).

[70] D. D. Beck, J. M. White, and C. T. Ratcliffe, Catalytic reduction of carbon monoxide with hydrogen sulfide. 2. Adsorption of water and hydrogen sulfide on anatase and rutile, J. Phys. Chem. **90**, 3123 (1986).

[71] R. Martinez-Casado, G. Mallia, N. M. Harrison, and R. Pérez, First-principles study of the water adsorption on anatase(101) as a function of the coverage, J. Phys. Chem. C **122**, 20736 (2018).

[72] N. Pueyo Bellafont, F. Viñes, W. Hieringer, and F. Illas, Predicting core level binding energies shifts: Suitability of the projector augmented wave approach as implemented in VASP, J. Comput. Chem. **38**, 518 (2017).

[73] D. Dvoranová, Z. Barbieriková, and V. Brezová, Radical intermediates in photoinduced reactions on TiO_2 (an EPR spin trapping study), Molecules **19**, 17279 (2014).

[74] J. Tang, J. R. Durrant, and D. R. Klug, Mechanism of photocatalytic water splitting in TiO_2. reaction of water with photoholes, importance of charge carrier dynamics, and evidence for four-hole chemistry, J. Am. Chem. Soc. **130**, 13885 (2008).

[75] E. G. Panarelli, S. Livraghi, S. Maurelli, V. Polliotto, M. Chiesa, and E. Giamello, Role of surface water molecules in stabilizing trapped hole centres in titanium dioxide (anatase) as monitored by electron paramagnetic resonance, J. Photochem. Photobiol. A **322–323**, 27 (2016).

[76] S. Selcuk and A. Selloni, Facet-dependent trapping and dynamics of excess electrons at anatase TiO_2 surfaces and aqueous interfaces, Nat. Mater. **15**, 1107 (2016).